Detection of a Weak Somatosensory Stimulus: Role of the Prestimulus Mu Rhythm and Its Top–Down Modulation

Yan Zhang and Mingzhou Ding

Abstract

■ The ongoing neural activity in human primary somatosensory cortex (SI) is characterized by field potential oscillations in the 7–13 Hz range known as the mu rhythm. Recent work has shown that the magnitude of the mu oscillation immediately preceding the onset of a weak stimulus has a significant impact on its detection. The neural mechanisms mediating this impact remain not well understood. In particular, whether and how somatosensory mu rhythm is modulated by executive areas prior to stimulus onset for improved behavioral performance has not been investigated. We addressed these issues by recording 128-channel scalp electroencephalogram from normal volunteers performing a somatosensory perception experiment in which they reported the detection of a near-threshold electrical stimulus (~50% detection rate) delivered to the right index finger. Three results were found. First, consistent with numerous previous reports, the N1 component (~140 msec) of the somatosensory-evoked potential was significantly enhanced for perceived stimulus compared to unperceived stimulus. Second, the prestimulus mu power and the evoked N1 amplitude exhibited an inverted-U relationship, suggesting that an intermediate level of prestimulus mu oscillatory activity is conducive to stimulus processing and perception. Third, a Granger causality analysis revealed that the prestimulus causal influence in the mu band from prefrontal cortex to SI was significantly higher for perceived stimulus than for unperceived stimulus, indicating that frontal executive structures, via ongoing mu oscillations, exert cognitive control over posterior sensory cortices to facilitate somatosensory processing. ■

INTRODUCTION

When a weak stimulus is presented to a human subject, it is sometimes perceived and sometimes not. This paradigm is often used to study the neuronal mechanisms of sensory perception and stimulus awareness. In the somatosensory domain, a main finding is that the amplitude of the stimulus-evoked N1 component (~140 msec) over primary somatosensory cortex (SI) is significantly higher for perceived than for unperceived stimulus (Schubert, Blankenburg, Lemm, Villringer, & Curio, 2006; Libet, Alberts, Wright, & Feinstei, 1967). Because the N1 component is thought to be generated by feedback from higher-order sensory (e.g., secondary somatosensory cortex, SII) and executive (e.g., prefrontal cortex, PFC) areas (Jones, Pritchett, Stufflebeam, Hamalainen, & Moore, 2007; Staines, Graham, Black, & McIlroy, 2002; Waberski, Gobbele, Darvas, Schmitz, & Buchner, 2002; Allison, McCarthy, & Wood, 1992; Desmedt & Tomberg, 1989), this finding is consistent with reversible lesion studies where the temporary disruption of neural feedback prevented stimulus perception (Jackson & Cauller, 1998). Moreover, the N1 amplitude is sensitive to attention requirement (Eimer & Forster, 2003; Nakajima & Imamura, 2000; Garcia-Larrea, Lukaszewicz, & Mauguiere, 1995; Desmedt & Robertson, 1977). This has led to the notion that top–down attentional signals from higher-order structures elicited by the stimulus input are an essential element of sensory perception (Golmayo, Nunez, & Zaborszky, 2003; Staines et al., 2002; Waberski et al., 2002; Posner & Petersen, 1990). In agreement with this idea, permanent damage to PFC results in a smaller evoked N1 component (Knight, Staines, Swick, & Chao, 1999).

The traditional view of sensory information processing and perception places emphasis on stimulus-evoked responses and their modulation by higher mental processes such as attention. More recent work has begun to elucidate the importance of ongoing brain activity immediately before stimulus onset in defining a state of the brain and the effect of such a state on subsequent stimulus processing (Dale, Simpson, Foxe, Luks, & Worden, 2008; Zhang, Wang, Bressler, Chen, & Ding, 2008; Dehaene & Changeux, 2005; Liang, Bressler, Ding, Truccolo, & Nakamura, 2002; Engel, Fries, & Singer, 2001). In somatosensory cortex, ongoing neural activity is dominated by oscillations in the 7–13 Hz range, called the mu rhythm. Although the precise function of the mu rhythm is still under debate (Pineda, 2005; Pfurtscheller, Neuper, Andrew, & Edlinger, 1997; Salenius, Schnitzler, Salmelin, Jousmaki, & Hari, 1997), there is increasing evidence that the mu rhythm was sensitive to changes in cognitive and attentional requirements, and is likely to play a significant role in stimulus processing (Klimesch, Sauseng, & Hanslmayr, 2007; Palva & Palva,

University of Florida, Gainesville

2007). In an MEG study, Linkenkaer-Hansen, Nikulin, Palva, Ilmoniemi, and Palva (2004) employed a weak electrical stimulus to reveal an inverted-U relationship between the magnitude of ongoing prestimulus mu activity and the subsequent probability of stimulus detection, suggesting that an intermediate level of prestimulus mu activity facilitates sensory processing. The neural mechanisms behind this relationship are not well understood. In particular, the question of whether and how other brain areas, particularly the executive areas in the frontal lobe, modulate the neural activity in the somatosensory area for improved behavioral performance has not been studied.

To address these issues, scalp electroencephalogram (EEG) was recorded from healthy human volunteers performing a sensory perception task in which they were instructed to respond to the onset of a near-threshold (~50% detection rate) electrical impulse delivered to the right index finger. The experiment has two objectives. First, in light of the significant role played by the N1 component in sensory perception, it is hypothesized that the N1 amplitude and the magnitude of the prestimulus mu oscillation should be related as an inverted-U function. The successful testing of this hypothesis is expected to shed light on the neural basis underlying the observed mu–behavior relationship reviewed earlier. Second, recent work in both humans and nonhuman primates has stressed the importance of biasing signals from PFC in modulating activities in sensory areas for improved behavioral performance (Engel et al., 2001; Miller & Cohen, 2001; Hopfinger, Buonocore, & Mangun, 2000; Kastner, Pinsk, De Weerd, Desimone, & Ungerleider, 1999). Applying the Granger causality method, we tested the hypothesis that enhanced N1 amplitude and stimulus detection is accompanied by stronger causal influence from prefrontal areas to somatosensory cortex during the prestimulus time period.

METHODS

Subjects

The experimental protocol was approved by the Institutional Review Board of the University of Florida. Seventeen right-handed subjects, free from movement and neurological disorders, were recruited. They signed informed consent and were paid $30 for their participation. Two subjects did not finish the experiment. One additional subject exhibited excessive movement and another fell asleep from time to time during the experiment. The remaining 13 subjects (24–38 years old, 3 women) performed the task according to instructions. Their behavioral and physiological data were further analyzed.

Behavioral Paradigm

Subjects sat comfortably in a wooden chair with their eyes closed and their arms rested on a table in front of them. Their right index finger was stimulated by a biphasic near-threshold electrical impulse (0.3 msec in duration and less than 3 mA in intensity) delivered via a pair of electrodes placed 2 cm apart on the distal (anode) and middle (cathode) phalanges. They were instructed to press a button on a response pad with the left index finger as soon as they felt the electrical stimulation. The stimulus intensity was adjusted to each individual's sensory threshold, that is, the intensity at which ~50% of the stimuli were perceived, using a procedure similar to the staircase method described by Leek (2001). Among all subjects, the maximal stimulus intensity was found to be less than 3 mA. The experiment consisted of 10 blocks, lasting about 50 min, with breaks given between blocks. Each block had 40 trials where the intertrial interval varied randomly from 4.5 to 5 sec. The stimulus intensity was kept the same throughout the experiment to avoid the intensity effect on the somatosensory-evoked potentials (SEPs; Nakajima & Imamura, 2000; Cauller & Kulics, 1991) and to enable the pooling of trials across blocks required by the subsequent analysis. Before the experiment, subjects were given at least 40 practice trials to minimize adaptation and learning effects.

EEG Recording

The experiment took place in an acoustically and electrically shielded booth. To reduce the effect of eye blinks and eye movements, and to avoid visual modulation of somatosensory processing (Taylor-Clarke, Kennett, & Haggard, 2002), subjects were asked to keep their eyes closed during the experiment. The EEG data were acquired by a 128-channel BioSemi ActiveTwo System (www.biosemi.com) with a sampling rate of 2048 Hz. Electrooculogram (EOG) for horizontal and vertical eye movement was monitored with four electrodes placed around the eyes. The EEG signal was off-line band-pass filtered between 0.3 and 50 Hz and down-sampled to 250 Hz. A Grass stimulator (model S48) was used to generate the stimulating electrical impulse and the response was recorded by a BeriSoft EXKEY microprocessor logic pad (www.berisoft.com).

Data Preprocessing

The time of stimulus onset was defined as 0 msec. The continuous EEG data were epoched from −500 to 1000 msec. Trials with EOG exceeding 100 μV or having incorrect response times (>2.5 sec or <0.15 sec) were excluded from further analysis (<1%). The EEG data were re-referenced against the average reference (Nunez et al., 1997). Data analysis was performed with BESA 5.0 (www.besa.com), MATLAB (www.mathworks.com), and custom Matlab software. In each subject, the location of left primary somatosensory area (SI), which was contralateral to the stimulated hand, was determined by the maximum positive deflection of the early SEP component P60 (50 to 70 msec), aided by the scalp current density (SCD) map (Scherg, Ille, Bornfleth, & Berg, 2002; Perrin, Pernier,

Bertrand, & Echallier, 1989). Two electrodes, typically 2 cm posterior to C3, were selected to represent the neural activity in SI, whereas the neural activity in PFC was represented by three electrodes, Fpz, Fp1, and Fp2 (see Figure 3A). Given the coarse spatial resolution of the scalp EEG, subdivisions of PFC are not resolved.

Behavior and Evoked Potential Analysis

The behavioral performance was measured by the stimulus detection rate which is defined as the number of correctly perceived stimuli divided by the total number of stimuli. This rate could be computed for the entire experiment, for a block or for a specific group of trials (see below). The SEP was computed in the conventional way. As the electrical stimulus delivered to the finger created a skin-conducted potential extending all the way to the scalp, and this potential was spread temporally by the band-pass filter used for data preprocessing, the data from −20 to 20 msec were considered unreliable. Two SEP components were analyzed: P60 (40–60 msec) and N1 (120–160 msec, also called N140). The amplitude of these SEP components was estimated using the baseline-to-peak method where the baseline period was defined to be (−100 msec, −20 msec) (Luck, 2005). The Wilcoxon signed-rank test was used to test whether the difference for each of the two components between the perceived and unperceived conditions is statistically significant.

Correlation between Prestimulus Mu Power and Stimulus Detection Rate

The prestimulus time window for mu power analysis was defined to be (−500 msec, −20 msec). For each subject, the average power in the mu frequency band (7–13 Hz) over the SI area for each trial in the prestimulus window was calculated for each of the two electrodes by the multitaper spectral analysis method (Mitra & Pesaran, 1999; Thomson, 1982) and was averaged over the two electrodes. The trials, pooled together from all blocks, were then rank ordered by the magnitude of the prestimulus mu power, from the smallest to the largest, and sorted into 10 groups of equal size (Zhang et al., 2008; Liang et al., 2002). The size of the group, ~18% of the total available trials, was chosen in such a way that it had half the trials overlapped with the previous group. The power groups were indexed from 1 to 10 where Group 1 has the smallest mu power and Group 10 has the largest (see Figure 1 for a schematic). In each power group, the stimulus detection rate was calculated for every subject. To minimize the effect of intersubject variability in detection rate on population averaging, the following procedure was adopted to normalize the data from each subject. Let the stimulus detection rate for Subject K in Power Group J be denoted by $\mathrm{DR}(K,J)$. The mean detection rate for this subject was $\mathrm{meanDR}(K) = [\mathrm{DR}(K,1) + \mathrm{DR}(K,2) + \ldots + \mathrm{DR}(K,10)]/10$. The normalized detection rate was measured by the percent change against this mean, namely, $\mathrm{normDR}(K,J) = (\mathrm{DR}(K,J) - \mathrm{meanDR}(K))/\mathrm{meanDR}(K)$. This normalized detection rate was then averaged over subjects to obtain the population mean normalized detection rate for each power group.

Correlation between Prestimulus Mu Power and N1 Amplitude

For each subject, the trials within a power group were used to calculate the SEP. The N1 amplitude for each subject was measured by the averaged SEP in a 40-msec interval centered on the maximum negative waveform deflection between 110 and 170 msec. As there is variability in N1 amplitude from subject to subject, to facilitate population averaging, the same normalization procedure above for stimulus detection rate was used to obtain the mean normalized N1 amplitude for each power group. In some analysis, only perceived trials in each power group were used to calculate the averaged SEP.

Granger Causality Analysis

Multivariate neural data are becoming commonplace. How to analyze these data to assess brain network operation underlying cognition presents a formidable challenge. Granger causality (Ding, Chen, & Bressler, 2006; Geweke, 1982; Granger, 1969) has emerged in recent years as a statistically principled method to calculate the direction of information transmission or driving (Bollimunta, Chen, Shroeder, & Ding, 2008; Chen, Bressler, & Ding, 2006; Brovelli et al., 2004; Kaminski, Ding, Truccolo, & Bressler, 2001). This technique was applied here to EEG time series to estimate the direction of synaptic transmission between the three prefrontal electrodes and the two SI electrodes during the prestimulus time period and its impact on stimulus

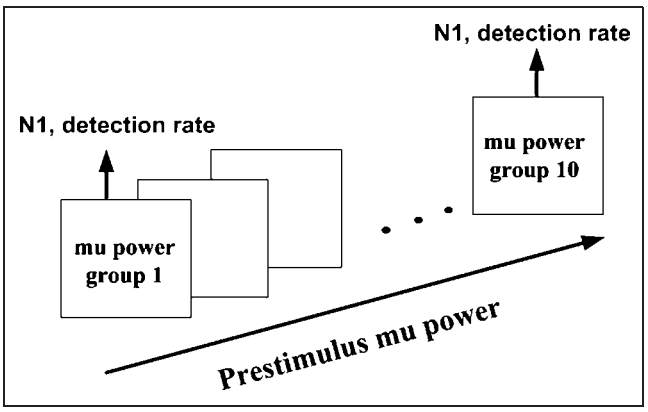

Figure 1. Schematic of the single-trial sorting procedure. Trials were rank ordered by the magnitude of prestimulus mu power over somatosensory cortex and then sorted into 10 groups of equal size. The group size, which corresponds to roughly 18% of the total number of trials, is such that each group has half the trials overlapped with the previous group. The groups defined this way are referred to mu power groups.

processing. Detailed mathematical formulation and associated interpretation were given in the Appendix. Briefly, consider two electrodes, one prefrontal and another SI, and an ensemble of trials during the prestimulus time period (−500 msec to −20 msec). The ensemble mean for each electrode was calculated and subtracted from each single trial to ensure that the data can be treated as coming from a zero-mean stochastic process (Ding, Bressler, Yang, & Liang, 2000). A bivariate autoregressive model was fit to the mean-corrected data from the two electrodes where the model order was chosen by the Akaike Information Criterion (Akaike, 1974). From the model, Granger causality spectra from the prefrontal electrode to the SI electrode (PFC → SI) and that for the opposite direction (SI → PFC) were derived. This process was repeated for each distinct PFC–SI electrode pair (6 in total) and the resulting six spectra were averaged for each direction.

Several questions were considered. First, was there a difference in prestimulus Granger causal influence in the mu band between the perceived and unperceived conditions? For each subject, the trials were divided into the perceived ensemble and the unperceived ensemble. Granger causality spectra were averaged in the mu band for both directions. As with any other physiological variables, Granger causality values varied markedly from subject to subject. To remove the possible adverse effect of this variability on population averaging, the causal influence for each condition was normalized by dividing the sum of causal influences from both conditions. The Wilcoxon signed-rank test was then applied to evaluate the statistical difference between the two conditions. Second, was PFC → SI influence in the mu band correlated with the N1 amplitude? For each subject, trials from a prestimulus power group formed an ensemble. Granger causality in the mu band and the N1 amplitude was extracted from each power group. The same normalization procedure based on the percent change against the mean was performed on the Granger causality and the result was plotted against the normalized N1 amplitude. Linear regression and Spearman's rank correlation were applied to assess the relation between the two variables. Third, what was the function linking prestimulus mu power and mu-band Granger causality? Here, the Granger causality in the mu frequency band was evaluated for each power group for each subject. The relationship was examined both individually and for a group of subjects.

Higher Frequency Activity

Neural activity in the beta (16–30 Hz) and gamma (30–45 Hz) frequency band was examined with the same analysis protocol outlined above, starting with the sorting of trials into 10 beta or gamma power groups based on the single-trial beta or gamma magnitude in the prestimulus time period. The dependence of the N1 amplitude on beta and gamma power was examined. In addition, Granger causality in each of the two bands was extracted and compared between perceived and unperceived trials.

RESULTS

Behavior

Thirteen subjects (n = 13) performed the task according to instructions. The rate of stimulus detection for each subject is shown in Figure 2A. The individual rate was found to be not significantly different from 50% (Wilcoxon signed-rank test, Bonferroni corrected, $p > .05$). The detection rate averaged across subjects (n = 13) gives 0.51 ± 0.01 (mean ± *SEM*). For each block (~5 min), the detection rate averaged across subjects (n = 13) is plotted as a function of block index in Figure 2B. Although the performance became more variable toward the end of the experiment, the detection rate at the individual block level was again found to be not significantly different from 50% (Wilcoxon signed-rank test, Bonferroni corrected, $p > .05$). For correctly detected stimulus, the median response time across all subjects was 612 msec.

Somatosensory-evoked Potential

After data preprocessing, there were, on average, 156 ± 12 perceived trials and 152 ± 13 unperceived trials available

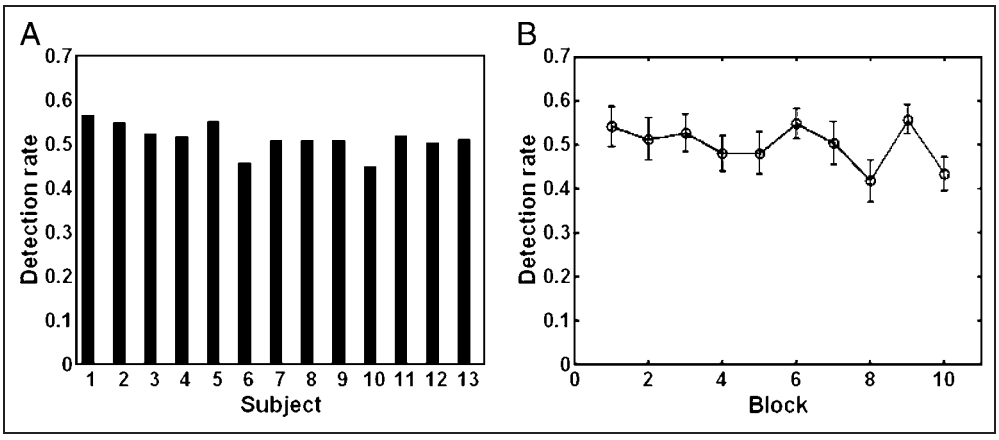

Figure 2. Behavioral results. (A) The height of each bar represents the probability of detecting a near-threshold stimulus for each subject (detection rate). (B) Detection rate in each experimental block was averaged across all 13 subjects and plotted against the block index. Error bars are standard error of the mean.

from each subject for further analysis. The grand-average (n = 13) SEP waveforms (0 to 200 msec) over the primary somatosensory cortex (SI) (Figure 3A) for perceived trials and unperceived trials are shown in Figure 3B. The N20 (20 to 40 msec) component was not per millisecond due to the small stimulus intensity and it was further distorted by the band-pass filtering of the skin-conducted stimulus artifact. It was not further investigated. The P60 (50 to 70 msec) component was clearly visible but its amplitude was not significantly different between perceived and unperceived trials (Wilcoxon signed-rank test, $p > .05$). In contrast, the amplitude of the N1 (120 to 160 msec, also called N140) component was significantly enhanced (Wilcoxon signed-rank test, $p < .00002$) for perceived trials as compared to unperceived trials. Two other components, N80 (70 to 95 msec) and P100 (100 to 120 msec), occurring between the P60 and the N1, were only observed in three or four subjects, and thus, were not investigated further. These ERP results, particularly the modulation of the N1 amplitude by stimulus perception, were consistent with previous studies (Schubert et al., 2006; Meador, Ray, Echauz, Loring, & Vachtsevanos, 2002; Libet et al., 1967). It is worth noting that Jones et al. (2007) and Palva, Linkenkaer-Hansen, Näätänen, and Palva (2005) reported perception-related modulation of earlier stimulus-evoked responses (60 to 100 msec). Their work is based on MEG data rather than EEG data.

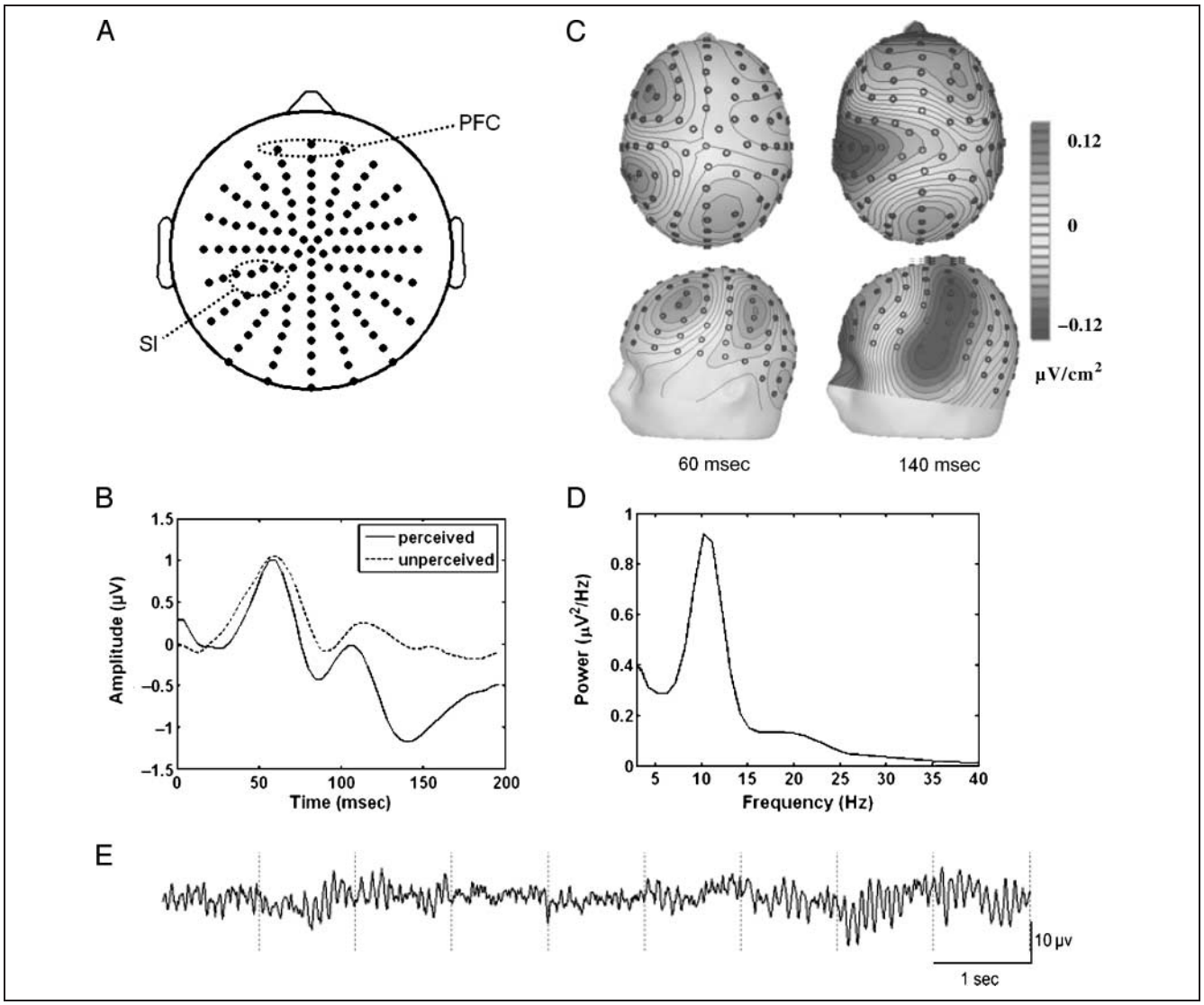

Figure 3. Electrode selection, SEP, and ongoing mu oscillations. (A) The three electrodes enclosed by the dashed oval labeled PFC were used to represent neural activity in prefrontal cortex. Two electrodes in the dashed oval labeled SI were chosen according to their P60 amplitude to represent neural activity in primary somatosensory cortex. (B) Grand-average SEPs for perceived (solid) and unperceived (dotted) trials over contralateral SI (left hemisphere). The N1 component (~140 msec) was significantly enhanced for perceived trials. (C) Scalp current source density maps of the grand-average SEPs at 60 and 140 msec (see text for details). The contour lines in SCD maps are separated by 0.01 μV/cm^2. (D) Power spectrum of prestimulus EEG data averaged over the two SI electrodes for one subject. (E) Spontaneous EEG time series showing mu oscillations during eye-closed rest for one subject.

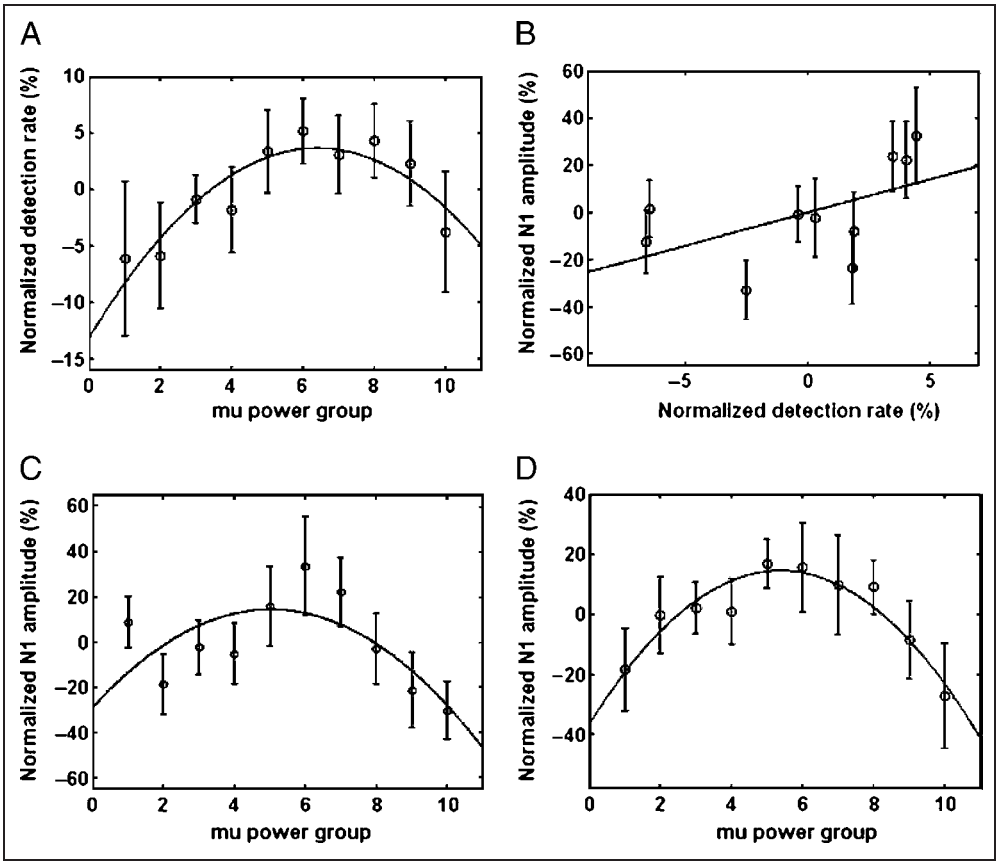

Figure 4. Relation between prestimulus ongoing mu oscillation and stimulus processing and detection. The solid lines represent either quadratic or linear fit. Error bars are standard error of the mean. (A) Stimulus detection rate versus prestimulus mu power (see Figure 1 and text for definition of mu power group). (B) Normalized N1 amplitude versus normalized detection rate. (C) Normalized N1 amplitude versus prestimulus mu power. (D) Normalized N1 amplitude versus prestimulus mu power where only perceived trials in each mu power group were used.

To examine the spatial topography of the P60 (Figure 3C, left column, two different views) and the N1 (Figure 3C, right column, two different views) components, SCD maps were derived and shown in Figure 3C. Both components are clearly lateralized to the left hemisphere. At 60 msec, a dipole pattern, with a current sink in the precentral area and a current source in the postcentral area, was seen. The location of the latter was used to aid the selection of the two electrodes to represent SI. At 140 msec, a large current sink is observable over both the pre- and postcentral areas, extending possibly into secondary somatosensory cortex.

The Mu Rhythm

Stimulus-evoked response is influenced by the ongoing brain activity prior to stimulus onset. Over SI, this ongoing activity is dominated by the mu rhythm, as demonstrated by the power spectrum from one subject in Figure 3D. Two features are noteworthy: (1) a prominent peak at around 10 Hz and (2) rapid decay of power at frequencies beyond 20 Hz (Salmelin & Hari, 1994). Similar features were observed in the power spectra from all 13 subjects. The peak frequencies ranged from 9 to 11 Hz (mean: 10.5 ± 0.7 Hz). A segment of spontaneous EEG from an SI electrode in one subject is shown in Figure 3E. Clearly, the mu amplitude (power) is not constant, and it fluctuates over time in a stochastic fashion. The waxing and waning of the mu rhythm was expected to have varied impact on the processing of sensory input.

Prestimulus Mu Power and Behavior

For each group of trials sorted according to the magnitude of prestimulus mu power (see Figure 1), the normalized rate of stimulus detection, defined as the averaged (n = 13) percent change of detection rate in a power group relative to the mean detection rate, was computed and plotted as a function of the group index in Figure 4A. An inverted-U relationship is readily identifiable. The solid curve is a quadratic fit which is highly significant (r^2 = .88, $p < .0006$). A linear regression model, however, failed to properly describe the data ($r^2 = .32, p = .1$). This finding is consistent with a previous report by Linkenkaer-Hansen et al. (2004) using MEG recordings.

Prestimulus Mu Power and N1 Amplitude

As seen above, the amplitude of the SEP N1 component is an important signature correlated with the correct perception of a weak stimulus. Two predictions can be made. First, the power group with a higher stimulus detection

rate should correspond to higher N1 amplitude. This predicted linear relationship was tested by plotting average normalized N1 amplitude against average normalized detection rate (n = 13). The result is shown in Figure 4B where a linear regression yielded r^2 = .35 (p = .06) and a Spearman rank correlation gave ρ = .62. Although the linear fit barely missed the significance level of .05, the trend is clearly discernible. The lack of an N1 component (see Figure 3B) in the unperceived trials within each power group contributed to the dilution, and thus, poor estimation of the N1 amplitude in Figure 4B. Second, the N1 amplitude should depend on the prestimulus mu power as an inverted-U function. This predicted nonlinear relationship was tested by plotting the average normalized N1 amplitude (n = 13) in each power group against the group index. The result is shown in Figure 4C. The solid curve is a quadratic fit which is statistically significant ($r^2 = .70, p < .01$). If only perceived trials were considered within each power group, the relationship becomes even stronger, as seen in Figure 4D ($r^2 = .88, p < .0006$). The reason for the improvement is that the N1 component appeared more reliably in the perceived trials. Quantitatively, the maximum N1 amplitude, occurring for Power Group 6 (intermediate mu power), is 32 ± 17% (mean ± *SEM*) or 44 ± 19% (mean ± *SEM*) higher than that in Power Groups 1 (lowest mu power) and 10 (highest mu power), respectively.

Higher Frequency Activity

The relationship between the N1 amplitude and the prestimulus ongoing neural oscillation in higher frequencies, namely, the beta (16–30 Hz) and gamma (30–45 Hz) band oscillation, was similarly investigated. No significant correlation of either the linear or quadratic type was found. It should be noted that the power of the beta and gamma activity is small relative to that of the mu activity. Thus, the single-trial estimation of these activities may not be as reliable as that of the mu activity. In addition, our assessment of the prestimulus brain state is less accurate for higher frequency activity due to the −20 to 20 msec exclusion zone.

Individual Subjects

The relationship between the prestimulus mu power and the N1 amplitude was further investigated at the individual subject level. Figure 5A displays the data from Subject 10 where a quadratic fit gave r^2 = .76 ($p < .006$) and a linear fit gave r^2 = .07 (p = .46). The p values from quadratic fitting to the data from all 13 subjects are shown in Figure 5B, together with the p values from linear fitting. For 9 out of 13 subjects (3, 5, 6, 7, 8, 9, 10, 11, and 12), the relationship between prestimulus mu power and N1 amplitude was well described by a quadratic regression model ($p < .05$) but not by a linear regression model ($p > .05$). For Subject 1,

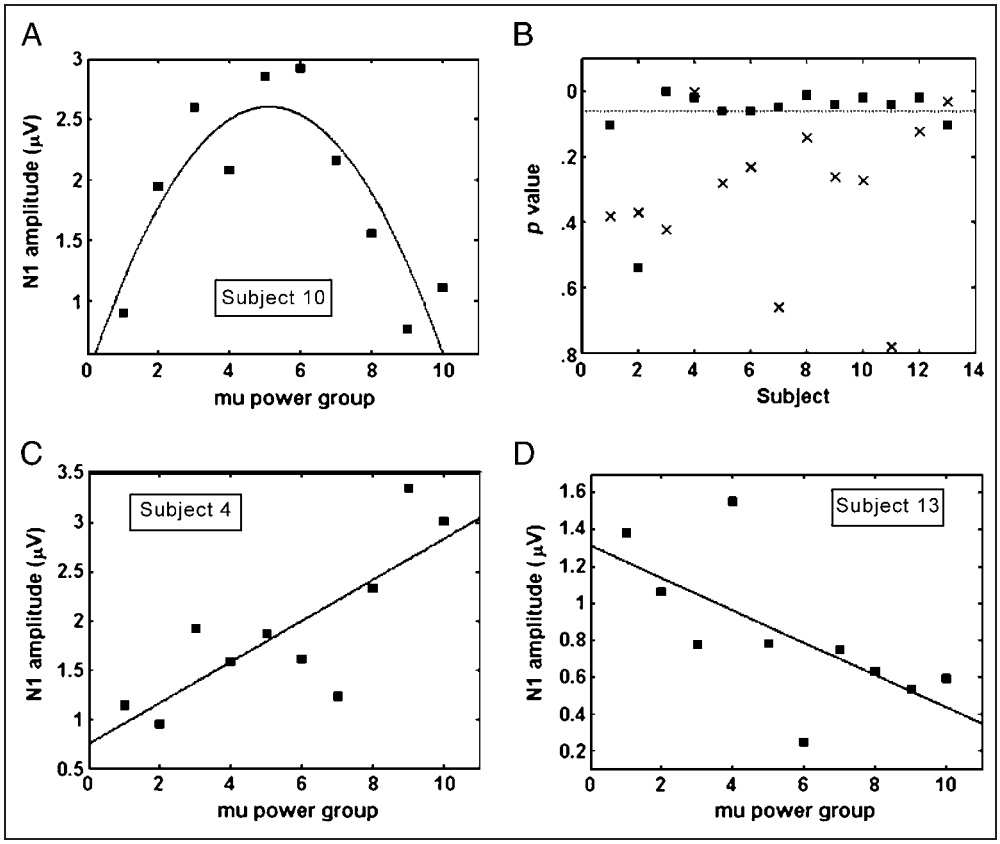

Figure 5. The N1 amplitude versus prestimulus mu power for individual subjects. Solid lines represent either quadratic or linear fit. (A) N1 amplitude versus prestimulus mu power for Subject 10. (B) The p values from quadratic (filled squares) and linear (×) fits for each of 13 subjects. The horizontal dotted line indicates the significance level of p = .05. (C) N1 amplitude versus prestimulus mu power for Subject 4. (D) N1 amplitude versus prestimulus mu power for Subject 13.

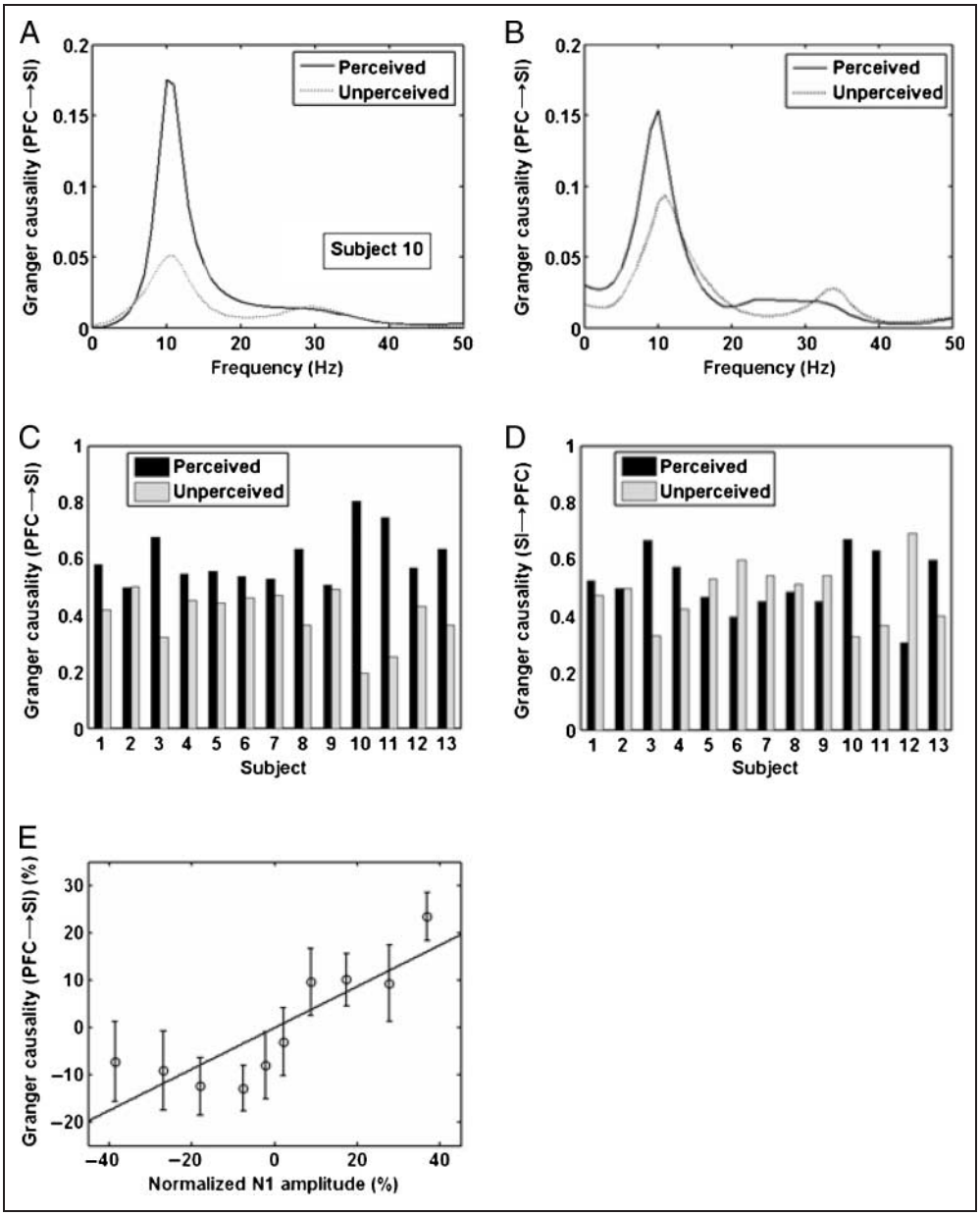

Figure 6. Effects of prestimulus Granger causal influence from PFC to SI (PFC → SI). (A) PFC → SI Granger causality spectra for perceived (solid) and unperceived (dashed) trials for Subject 10. (B) PFC → SI Granger causality spectrum averaged across 13 subjects. (C) and (D) PFC → SI and SI → PFC averaged over mu band for perceived (black) and unperceived (gray) trials for each of the 13 subjects. (E) PFC → SI in mu band versus N1 amplitude. Solid line represents a linear fit. Error bars are standard error of the mean.

although the p value from the quadratic fit did not reach significance, the N1 amplitude for an intermediate power group (Group 6) was about 50% greater than that for the lowest and highest power groups. Thus, the data for this subject can still be considered as following an inverted-U relationship. The remaining three subjects (2, 4, and 13) presented three distinctively different patterns. For Subject 4, this relationship is linear with a positive slope (linear regression, $r^2 = .74, p < .001$; Figure 5C), whereas for Subject 13, the relationship is again linear, but with a negative slope (linear regression, $r^2 = .45, p < .03$; Figure 5D). As the inverted-U function has both a monotonically increasing segment (to the left of the maximum) and a monotonically decreasing segment (to the right of the maximum), the two linear relationships with opposite slopes may indicate that the mu activity in these two subjects concentrated only in the respective linear ranges, and did not extend to the full range underlying their individual inverted-U functions. For Subject 2, no significant relationship of either the quadratic or the linear type was found (linear regression, $r^2 < .32, p > .08$).

Causal Influences between PFC and SI

The foregoing demonstrated that the magnitude of the prestimulus ongoing mu activity in the somatosensory area can impact stimulus processing. The question of whether this prestimulus activity was subjected to the top–down modulation by prefrontal executive structures for enhanced behavioral performance was investigated by computing the Granger causality spectra between the three prefrontal electrodes and the two SI electrodes. Figure 6A shows the result contrasting perceived versus unperceived conditions for Subject 10. The grand-average

spectrum is shown in Figure 6B ($n = 13$). It is clear that PFC → SI influence was substantially higher for perceived trials than for unperceived trials in the mu band. Figure 6C shows PFC → SI averaged over the mu band for each of the 13 subjects for both perceived and unperceived trials. PFC → SI causal influence for perceived trials was significantly higher (Wilcoxon signed-rank test, $p < .001$) than that for unperceived trials over the population of 13 subjects.

Three additional causal influences were investigated: (1) SI → PFC in the mu band, (2) causal influences in higher frequencies in both directions, and (3) causal influence from the prefrontal executive structures to visual cortex (control condition). First, as seen in Figure 6D, the difference in SI → PFC between perceived and unperceived trials was not consistent across subjects. Specifically, 6 of the 13 subjects had higher SI → PFC in the mu band for perceived trials, whereas the other 7 subjects had lower SI → PFC for perceived trials. A Wilcoxon signed-rank test yielded $p = .50$. Second, the Granger causal influence between PFC and SI in higher frequency range (>16 Hz and <45 Hz) was found to be not significantly different between the two conditions over the population of 13 subjects (data not shown). Third, as a control to examine the regional specificity of the top–down modulation in relation to behavior, Granger causal influence from the three prefrontal electrodes to visual cortical areas represented by the electrode Oz was evaluated in the mu frequency band. No significant difference between perceived and unperceived trials was found (Wilcoxon signed-rank test, $p = .12$), suggesting that, for the present experiment, the facilitating effect of the top–down influence is specific to the somatosensory domain.

For a given stimulus, if PFC → SI influence in the mu band was enhanced prior to its onset, it was more likely to be perceived. Two predictions can be made. First, considering the importance of the N1 component in indexing sensory perception and stimulus awareness, the magnitude of the prestimulus PFC → SI influence was expected to be positively correlated with the N1 amplitude. To test this idea, the average normalized mu-band PFC → SI influence and the average normalized N1 amplitude ($n = 13$) were calculated for the perceived trials in each power group and plotted in Figure 6E. A linear relationship was found ($r^2 = .72$, $p < .005$) where a Spearman rank correlation gave $\rho = .79$. Second, given that the N1 amplitude has an inverted-U dependence on prestimulus mu power, PFC → SI causal influence was expected to have the same inverted-U relationship with prestimulus mu power. Figure 7A displays the data from Subject 10 (see Figure 5A), where a quadratic fit yielded $r^2 = .73$ ($p < .01$). The normalized Granger causality in the mu band averaged over the nine subjects (3, 5, 6, 7, 8, 9, 10, 11, and 12) with $p < .05$ from the quadratic fit in Figure 5B as shown in Figure 7B. Again, a quadratic function describes the data well ($r^2 = .81$, $p < .003$), suggesting that stronger PFC → SI influence was associated with intermediate levels of prestimulus mu power, which in turn gave rise to higher N1

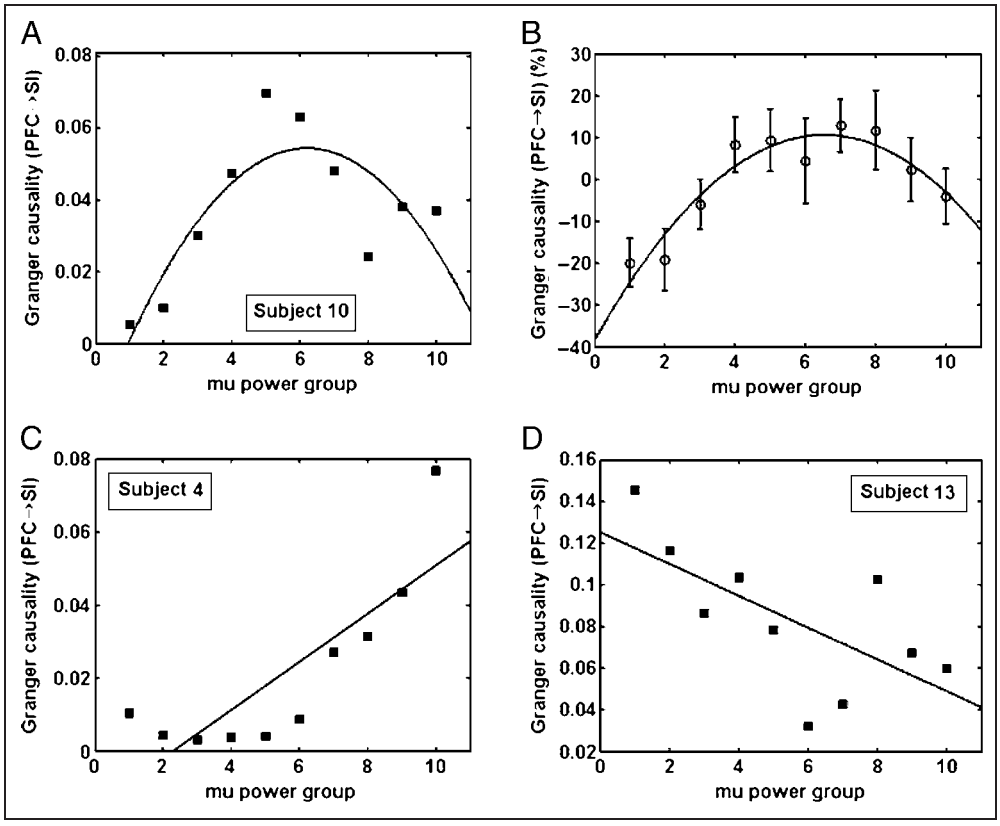

Figure 7. Relationship between prestimulus PFC → SI causal influence in mu band and prestimulus mu power over somatosensory cortex. Solid lines represent either quadratic or linear fit. (A) Subject 10. (B) Normalized mu band PFC → SI causal influence averaged across nine subjects with $p < .05$ from quadratic fit in Figure 5 (B). (C) Subject 4. (D) Subject 13.

amplitude and stimulus detection rate. The data from Subject 1 appeared to have similar inverted-U dependence, although it was not well fit by a quadratic function. For Subjects 4 and 13 shown in Figure 5C and D, the relationship is linear as expected, with a positive (linear regression fit, $r^2 = 0.75, p < .001$) and a negative slope (linear regression fit, $r^2 = .48, p < .03$), respectively (see Figure 7C and D). It is worth noting that, for these two subjects, stronger prestimulus PFC → SI influence also led to improved stimulus processing and detection. For Subject 2, no relationship of any type was found.

DISCUSSION

Scalp EEG was recorded from human subjects performing a sensory perception experiment in which they reported the detection of a weak electrical stimulus delivered to their right index finger. The intensity of the stimulus was chosen in such a way that it was correctly perceived approximately 50% of the time (near-threshold). Three results were found. First, the amplitude of the N1 component of the SEP is significantly higher for perceived than for unperceived stimulus. Second, the magnitude of the ongoing prestimulus mu oscillation (7–13 Hz) is correlated with the N1 amplitude as an inverted-U function, suggesting that intermediate levels of prestimulus mu activity lead to enhanced sensory processing and perception. Third, higher N1 amplitude and stimulus detection rate are preceded by increased prestimulus causal influence in the mu band from PFC to SI, supporting the notion that top–down executive control serves to bias input processing for enhanced behavioral performance.

Somatosensory-evoked Potential and Stimulus Processing

Two SEP components, P60 and N1, were investigated. They have distinct physiological origins and response characteristics. The P60 component (50 to 70 msec) is believed to be generated by an inhibitory postsynaptic potential near the somata of pyramidal cells in the deep layers (Wikstrom et al., 1996) of SI, and is mainly affected by stimulus parameters, even though it is known to be also slightly modulated by cognitive factors (Tomberg & Desmedt, 1996). The N1 component (120 to 160 msec) is a negative SEP deflection peaking around 140 msec poststimulus onset. It is thought to be partly generated by excitatory feedback inputs to SI from higher-order cortices, including secondary somatosensory cortex (SII), PFC, and posterior parietal cortex (Golmayo et al., 2003; Staines et al., 2002; Cauller, Clancy, & Connors, 1998; Jackson & Cauller, 1998; Cauller, 1995; Cauller & Kulics, 1991), and has a generator in the superficial layers of SI. In animal models, it has been shown that the N1 component is accompanied by increased action potential firing (Cauller & Kulics, 1991; Kulics & Cauller, 1986). Past work has shown that the N1 component is sensitive to both exogenous factors, such as stimulus intensity, and endogenous factors, such as selective attention and stimulus awareness (Schubert et al., 2006; Nakajima & Imamura, 2000; Garcia-Larrea et al., 1995; Desmedt & Robertson, 1977).

In the present experiment, the P60 component is found to be not affected by stimulus perception, whereas the N1 component is significantly higher for perceived trials than for unperceived trials (Figure 3B). This difference may be attributable to two factors: (1) these components reflect the activity of different neuronal populations, as indicated above and (2) their respective generation was mediated by distinct glutamate receptors. Recent proposals suggest that early evoked potential components rely more on the activation of alpha-amino-3-hydroxy-5-methyl-4-isoxazolepropionic acid receptors (AMPA), whereas late components (>100 msec) rely more on the activation of *N*-methyl-D-aspartic acid (NMDA) receptors (da Rocha, Pereira, & Coutinho, 2001; Salin & Bullier, 1995; Armstrongjames, Welker, & Callahan, 1993; McCarley, Faux, Shenton, Nestor, & Adams, 1991). Although the role of the AMPA receptors in sensory information coding has been well documented (Hollmann & Heinemann, 1994), more recent reports indicate that NMDA receptors in neocortex play a key role in higher mental processes such as sensory perception and memory formation (Vertes, 2005; Kochan, Churn, Omojokun, Rice, & Delorenzo, 2000; Newcomer et al., 1999). As feedback inputs target the superficial layers in neocortex (Felleman & Van Essen, 1991), the observed strong N1 response in perceived trials benefits from the denser distribution of NMDA receptors in the superficial layers (Cotman, Monaghan, Ottersen, & Stormmathisen, 1987; Greenamyre, Olson, Penney, & Young, 1985).

Prestimulus Ongoing Mu Rhythm and Stimulus Processing

Numerous in vitro or in vivo studies have demonstrated that spontaneous neural oscillations in the 5–20 Hz range can influence the timing and integration of sensory input (Lakatos, Chen, O'Connell, Mills, & Schroeder, 2007; Schaefer, Angelo, Spors, & Margrie, 2006; Lakatos et al., 2005; Vertes, 2005; Bland, Konopacki, & Dyck, 2002; Desmaisons, Vincent, & Lledo, 1999). In the present study, the prestimulus mu power is shown to have an inverted-U relationship with the N1 amplitude (Figure 4C and D). What is the neural process that links prestimulus oscillation with stimulus evoked response? Physiologically, spontaneous oscillations reflect a depolarizing drive on principle cells (Vertes, 2005; McCormick et al., 2003; Shu, Hasenstaub, Badoual, Bal, & McCormick, 2003; Destexhe & Pare, 1999). Input-related release of glutamate, when coupled with episodes of spontaneous oscillations, leads to more vigorous activation. Thus, the absence or very low levels of spontaneous oscillatory activity may fail to bring local neuron populations closer to firing threshold,

resulting in weak sensory-evoked response. In contrast, excessive levels of spontaneous oscillations, which are likely to be accompanied by more vigorous action potential firing, can lead to reduced sensory-evoked response (Dehaene & Changeux, 2005; Petersen, Hahn, Mehta, Grinvald, & Sakmann, 2003). Prolonged periods of elevated spiking preceding sensory input can result in: (1) short-term depression of excitatory synapses by depletion of synaptic vesicles (Chung, Li, & Nelson, 2002; Petersen, 2002; Zucker & Regehr, 2002; Galarreta & Hestrin, 1998; Abbott, Varela, Sen, & Nelson, 1997) and (2) increased inhibitory synaptic influence by activation of a subset of GABAergic interneurons surrounding the excitatory neuronal population (Galarreta & Hestrin, 1998; Markram, Wang, & Tsodyks, 1998; Reyes et al., 1998). These observations suggest that there is an intermediate level of oscillatory activity that is conducive to effective stimulus processing and subsequent perception. This idea has further support in recent slice and simulation work which has shown that a moderate amount of spontaneous synaptic background activity makes local neuron populations more sensitive to weak stimuli (Ho & Destexhe, 2000; Destexhe & Pare, 1999).

The amplitude of P60 is minimally affected by prestimulus mu activity (Nikouline et al., 2000) (data not shown). This may have two possible causes. First, the neuronal population supporting the mu activity and that giving rise to the P60 component are different. Second, in vitro studies have shown that oscillatory activity in the mu frequency range is closely associated with the facilitation of the NMDA receptors (Flint & Connors, 1996; Silva, Amitai, & Connors, 1991). As indicated above, the generation of the early SEP component P60 may be largely mediated by the AMPA receptors. This second point further explains the strong coupling between the prestimulus mu rhythm and the stimulus-evoked N1 component, which is known to depend on the activation of the NMDA receptors (da Rocha et al., 2001; Salin & Bullier, 1995; Armstrongjames et al., 1993; McCarley et al., 1991).

In addition to the amplitude, the phase of prestimulus oscillations can also significantly affect stimulus processing and the magnitude of the evoked potential (Lakatos, Karmos, Mehta, Ulbert, & Schroeder, 2008; Barry et al., 2004; Makeig et al., 2002; Jansen & Brandt, 1991). In visual cortex, Jansen and Brandt (1991) demonstrated that trials with a positive-going zero-crossing at stimulus onset had higher N1 amplitudes, whereas trials having negative-going zero-crossing had lower N1 amplitudes. For the present study, it is likely that for a given level of mu power, trials with certain phase values at stimulus onset will lead to a higher probability of stimulus detection. However, for each power group, as the intertrial intervals were varied randomly over a wide range (4.5 to 5 sec), the phase at stimulus onset is uniformly distributed from 0 to 2π, ensuring that between different power groups, the phase variable is controlled. The only variable remaining is the oscillation amplitude. In this sense, what was studied here is the effect of the amplitude of the prestimulus oscillation on stimulus processing and evoked response, with the phase removed as a potential confound.

Top–Down Modulation of Prestimulus Mu Rhythm and Stimulus Perception

The mu activity in somatosensory cortex prior to stimulus onset was shown to have a significant impact on stimulus processing and perception. What is the role played by other brain areas? It has been hypothesized that the prefrontal executive areas can exert a biasing influence on sensory cortices before stimulus input to enhance performance (Engel et al., 2001; Miller & Cohen, 2001; Hopfinger et al., 2000; Kastner et al., 1999). This idea was tested by measuring Granger causal influence between the prefrontal electrodes and the SI electrodes during the prestimulus time period. PFC → SI influence in the mu band is significantly higher for the perceived stimulus than for the unperceived stimulus (Figure 6C). No consistent results were found between perception and prestimulus SI → PFC influence (Figure 6D). In addition, prestimulus Granger causal influence in higher frequencies (beta and gamma band) is found to be not correlated with the rate of stimulus detection. These results are consistent with a recent proposal that lower frequency synchronization (e.g., mu or alpha) is more likely to be acclimated to the large-scale top–down processing, whereas the higher frequency neural oscillations is more suited for the stimulus-driven bottom–up processing in local networks (Buschman & Miller, 2007; Engel et al., 2001; Kopell, Ermentrout, Whittington, & Traub, 2000; von Stein, Chiang, & Konig, 2000; Gray, Konig, Engel, & Singer, 1989; Gray & Singer, 1989).

The somatosensory N1 component is known to be enhanced by the top–down influence from the anterior attention system including prefrontal and anterior cingulate cortices (Waberski et al., 2002; Allison et al., 1992; Desmedt & Tomberg, 1989). A lack of executive control in neurological patients with prefrontal lesions leads to reduced N1 amplitude (Knight et al., 1999; Chao & Knight, 1998; Knight, 1997). However, the event-related potential method employed in the previous studies cannot address the issue of whether the top–down facilitation is triggered by stimulus input or is implemented by the ongoing neural activity prior to stimulus onset. Our results provide strong evidence supporting a role of the latter. In particular, the positive correlation between the prestimulus PFC → SI causal influence in the mu band and the N1 amplitude (Figure 6E) establishes that the 10-Hz oscillatory activity is the carrier of the top–down biasing influence. It is worth noting that, the role of top–down influence is conventionally studied via lesion techniques, permanent or reversible (Gazzaley & D'Esposito, 2007; Rossi, Bichot, Desimone, & Ungerleider, 2007; Knight et al., 1999). The Granger causality method offers a complementary way of examining the role of top–down influence in a nonlesion

setting. This method has the additional benefit of being able to identify the neural signal that implements such influence.

How does the top–down signal achieve its optimizing effect? Physiologically, weak or strong ongoing mu rhythm reflects either an insufficient or excessive levels of neural excitation in SI. Both states are not conducive for effective stimulus processing. Not surprisingly, both states are associated with smaller PFC → SI causal influence, as seen in Figure 7A and B, for 10 out of 13 subjects (including Subject 1). The association between the strongest top–down causal influence and an intermediate level of ongoing mu oscillation suggests that the top–down facilitation is accomplished via either increased excitatory drive or increased inhibitory drive into the sensory cortices; the former when the local mu activity is too weak, whereas the latter when it is too strong. This idea has support in lesion data (Knight et al., 1999) showing that PFC's effect over posterior sensory and association cortices can be excitatory as well as inhibitory. A comparison between Figure 5C and D, and Figure 7C and D further reveals that, for the two subjects exhibiting linear relationships between prestimulus PFC → SI influence and mu power, stronger PFC → SI causal influence is associated with regions of mu activity that led to enhanced stimulus processing. Thus, individually, except for one subject (Subject 2), where no significant results of any kind were found, PFC → SI influence in the mu band is positively correlated with the quality of sensory processing and perception in 12 out of 13 subjects (92%).

Granger causality is a relative new method in EEG analysis. A few remarks on the technical aspect of its application are in order. First, one set of three electrodes and another set of two electrodes are used to represent prefrontal and SI activities, respectively. Similar effects are observed for electrodes near the selected sets. Second, both raw EEG time series re-referenced against the average reference and single-trial current source density data obtained through Laplacian procedures have been used in functional connectivity analysis. Their pros and cons are debated (Nunez et al., 1999). In this study, application of the Granger causality method to raw EEG time series was found to yield physiologically interpretable results. Two factors may contribute to this outcome. (1) The prefrontal electrodes and the SI electrodes are sufficiently apart so that their sharing of the same cortical sources is minimized. (2) The interdependence between two signals (A and B) can be decomposed into the sum of three components: A → B, B → A, and instantaneous causality resulting from both A and B receiving a common input with no significant relative time delay (Rajagovindan & Ding, 2008; Ding et al., 2006; Geweke, 1982). Volume conduction is mainly contained in instantaneous causality and has little effect on A → B and B → A. Third, functional connectivity analysis may ideally be performed in the source space. Although identifying cortical ERP generators is a mature field, source modeling of single-trial EEG data is less developed. Vigorous efforts along this direction are currently underway.

APPENDIX

Mathematical Formulation

Let the EEG time-series recordings from a prefrontal electrode and an SI electrode at time t be denoted by $\mathbf{X}_t = (x_{1t}, x_{2t})^T$ where T stands for matrix transposition. Assume that the data over the prestimulus time window are described by a bivariate autoregressive model:

$$\sum_{k=0}^{m} \mathbf{A}_k \mathbf{X}_{t-k} = \mathbf{E}_t \tag{1}$$

where $\mathbf{E}_t$ is a temporally uncorrelated residual error series with covariance matrix $\mathbf{\Sigma}$, and $\mathbf{A}_k$ are 2×2 coefficient matrices to be estimated from data (Ding et al., 2000). The model order m was determined by the Akaike (1974) Information Criterion (AIC), which reflects a trade-off between sufficient spectral resolution and overparameterization. For the data analyzed, m varied from subject to subject, the range being 10 to 18. Once the model coefficients $\mathbf{A}_k$ and $\mathbf{\Sigma}$ are estimated, the spectral matrix can be evaluated as:

$$\mathbf{S}(f) = \mathbf{H}(f)\mathbf{\Sigma}\mathbf{H}^*(f) \tag{2}$$

where the asterisk denotes matrix transposition and complex conjugation and $\mathbf{H}(f) = (\Sigma_{k=0}^{m} \mathbf{A}_k e^{-2\pi i k f})^{-1}$ is the transfer function. The Granger causality spectrum from x_{2t} to x_{1t} is defined as (Brovelli et al., 2004; Geweke, 1982):

$$I_{2\to 1}(f) = -\ln\left(1 - \frac{\left(\Sigma_{22} - \frac{\Sigma_{12}^2}{\Sigma_{11}}\right)|H_{12}(f)|^2}{S_{11}(f)}\right) \tag{3}$$

which can be interpreted as the proportion of x_{2t}'s causal contribution to the power of the x_{1t} series at frequency f. The logarithm is taken to preserve certain favorable statistical properties. Similarly, the causality spectrum from x_{1t} and x_{2t} can be obtained by switching the indices 1 and 2 in Equation 3. To obtain the causality value in a given frequency band, the above spectrum was averaged over the frequencies in the band.

Interpretation

Statistically, for two simultaneously measured time series, one series can be called causal to the other if we can better predict the second series by incorporating past knowledge of the first one (Wiener, 1956). This concept was formalized by Granger (1969) in the context of linear regression

models of stochastic processes (see Equation 1). Specifically, if the variance of the prediction error for the second time series at the present time is reduced by including past measurements from the first time series in the linear regression model, then the first time series can be said to have a causal (directional or driving) influence on the second time series. Reversing the roles of the two time series, one repeats the process to address the question of causal influence in the opposite direction. From this definition, it is clear that the flow of time plays an essential role in allowing inferences to be made about directional causal influences from time-series data. Alternatively, improvement in prediction can also be viewed from the perspective of comparing relative estimates of conditional probability. Recent work has modeled the relation between multiple point processes along this view (Okatan, Wilson, & Brown, 2005; Truccolo, Eden, Fellows, Donoghue, & Brown, 2005). In our analysis, the single-trial EEG data rereferenced against the average reference constitute the time series, and Granger causal influence is equated with the direction of synaptic transmission between neuronal ensembles (Bollimunta et al., 2008).

Reprint requests should be sent to Mingzhou Ding, The J. Crayton Pruitt Family Department of Biomedical Engineering, University of Florida, Gainesville, FL 32611, or via e-mail: mding@bme.ufl.edu.

REFERENCES

Abbott, L. F., Varela, J. A., Sen, K., & Nelson, S. B. (1997). Synaptic depression and cortical gain control. *Science, 275,* 220–224.

Akaike, H. (1974). New look at statistical-model identification. *IEEE Transactions on Automatic Control, AC-19,* 716–723.

Allison, T., McCarthy, G., & Wood, C. C. (1992). The relationship between human long-latency somatosensory evoked-potentials recorded from the cortical surface and from the scalp. *Electroencephalography and Clinical Neurophysiology, 84,* 301–314.

Armstrongjames, M., Welker, E., & Callahan, C. A. (1993). The contribution of NMDA and non-NMDA receptors to fast and slow transmission of sensory information in the rat Sl barrel cortex. *Journal of Neuroscience, 13,* 2149–2160.

Barry, R. J., Rushby, J. A., Johnstone, S. J., Clarke, A. R., Croft, R. J., & Lawrence, C. A. (2004). Event-related potentials in the auditory oddball as a function of EEG alpha phase at stimulus onset. *Clinical Neurophysiology, 115,* 2593–2601.

Bland, B. H., Konopacki, J., & Dyck, R. H. (2002). Relationship between membrane potential oscillations and rhythmic discharges in identified hippocampal theta-related cells. *Journal of Neurophysiology, 88,* 3046–3066.

Brovelli, A., Ding, M., Ledberg, A., Chen, Y., Nakamura, R., & Bressler, S. L. (2004). Beta oscillations in a large-scale sensorimotor cortical network: Directional influences revealed by Granger causality. *Proceedings of the National Academy of Sciences, U.S.A., 101,* 9849–9854.

Bollimunta, A., Chen, Y., Shroeder, C. E., & Ding, M. (2008). Neuronal mechanisms of cortical alpha oscillations in awake-behaving macaques. *Journal of Neuroscience, 28,* 9976–9988.

Buschman, T. J., & Miller, E. K. (2007). Top–down versus bottom–up control of attention in the prefrontal and posterior parietal cortices. *Science, 315,* 1860–1862.

Cauller, L. (1995). Layer I of primary sensory neocortex: Where top–down converges upon bottom–up. *Behavioural Brain Research, 71,* 163–170.

Cauller, L. J., Clancy, B., & Connors, B. W. (1998). Backward cortical projections to primary somatosensory cortex in rats extend long horizontal axons in layer I. *Journal of Comparative Neurology, 390,* 297–310.

Cauller, L. J., & Kulics, A. T. (1991). The neural basis of the behaviorally relevant N1 component of the SEP in SI cortex of awake monkeys—Evidence that backward cortical projections signal conscious touch sensation. *Experimental Brain Research, 84,* 607–619.

Chao, L. L., & Knight, R. T. (1998). Contribution of human prefrontal cortex to delay performance. *Journal of Cognitive Neuroscience, 10,* 167–177.

Chen, Y., Bressler, S. L., & Ding, M. (2006). Frequency decomposition of conditional Granger causality and application to multivariate neural field potential data. *Journal of Neuroscience Methods, 150,* 228–237.

Chung, S., Li, X. R., & Nelson, S. B. (2002). Short-term depression at thalamocortical synapses contributes to rapid adaptation of cortical sensory responses in vivo. *Neuron, 34,* 437–446.

Cotman, C. W., Monaghan, D. T., Ottersen, O. P., & Stormmathisen, J. (1987). Anatomical organization of excitatory amino-acid receptors and their pathways. *Trends in Neurosciences, 10,* 273–280.

da Rocha, A. F., Pereira, A., & Coutinho, F. A. B. (2001). *N*-methyl-D-aspartate channel and consciousness: From signal coincidence detection to quantum computing. *Progress in Neurobiology, 64,* 555–573.

Dale, C. L., Simpson, G. V., Foxe, J. J., Luks, T. L., & Worden, M. S. (2008). ERP correlates of anticipatory attention: Spatial and non-spatial specificity and relation to subsequent selective attention. *Experimental Brain Research, 188,* 45–62.

Dehaene, S., & Changeux, J. P. (2005). Ongoing spontaneous activity controls access to consciousness: A neuronal model for inattentional blindness. *PLoS Biology, 3,* 910–927.

Desmaisons, D., Vincent, J. D., & Lledo, P. M. (1999). Control of action potential timing by intrinsic subthreshold oscillations in olfactory bulb output neurons. *Journal of Neuroscience, 19,* 10727–10737.

Desmedt, J. E., & Robertson, D. (1977). Differential enhancement of early and late components of cerebral somatosensory evoked-potentials during forced-paced cognitive tasks in man. *Journal of Physiology (London), 271,* 761–782.

Desmedt, J. E., & Tomberg, C. (1989). Mapping early somatosensory evoked-potentials in selective attention: Critical-evaluation of control conditions used for titrating by difference the cognitive P-30, P40, P100 and N140. *Electroencephalography and Clinical Neurophysiology, 74,* 321–346.

Destexhe, A., & Pare, D. (1999). Impact of network activity on the integrative properties of neocortical pyramidal neurons in vivo. *Journal of Neurophysiology, 81,* 1531–1547.

Ding, M., Chen, Y., & Bressler, S. L. (2006). Granger causality: Basic theory and application to neuroscience. In B. Schelter, N. Winterhalder, & J. Timmer (Eds.), *Handbook of time series analysis* (pp. 437–460). Weinheim: Wiley–VCH Verlag.

Ding, M. Z., Bressler, S. L., Yang, W. M., & Liang, H. L. (2000). Short-window spectral analysis of cortical

event-related potentials by adaptive multivariate autoregressive modeling: Data preprocessing, model validation, and variability assessment. *Biological Cybernetics, 83,* 35–45.
Eimer, M., & Forster, B. (2003). Modulations of early somatosensory ERP components by transient and sustained spatial attention. *Experimental Brain Research, 151,* 24–31.
Engel, A. K., Fries, P., & Singer, W. (2001). Dynamic predictions: Oscillations and synchrony in top–down processing. *Nature Reviews Neuroscience, 2,* 704–716.
Felleman, D. J., & Van Essen, D. C. (1991). Distributed hierarchical processing in the primate cerebral cortex. *Cerebral Cortex, 1,* 1–47.
Flint, A. C., & Connors, B. W. (1996). Two types of network oscillations in neocortex mediated by distinct glutamate receptor subtypes and neuronal populations. *Journal of Neurophysiology, 75,* 951–956.
Galarreta, M., & Hestrin, S. (1998). Frequency-dependent synaptic depression and the balance of excitation and inhibition in the neocortex. *Nature Neuroscience, 1,* 587–594.
Garcia-Larrea, L., Lukaszewicz, A. C., & Mauguiere, F. (1995). Somatosensory responses during selective spatial attention—The N120-to-N140 transition. *Psychophysiology, 32,* 526–537.
Gazzaley, A., & D'Esposito, M. (2007). Top–down modulation and normal aging. *Imaging and the Aging Brain, 1097,* 67–83.
Geweke, J. F. (1982). Measurement of linear dependence and feedback between multiple time series. *Journal of the American Statistical Association, 77,* 304–313.
Golmayo, L., Nunez, A., & Zaborszky, L. (2003). Electrophysiological evidence for the existence of a posterior cortical–prefrontal–basal forebrain circuitry in modulating sensory responses in visual and somatosensory rat cortical areas. *Neuroscience, 119,* 597–609.
Granger, C. W. J. (1969). Investigating causal relations by econometric models and cross-spectral methods. *Econometrica, 37,* 424–438.
Gray, C. M., Konig, P., Engel, A. K., & Singer, W. (1989). Oscillatory responses in cat visual-cortex exhibit inter-columnar synchronization which reflects global stimulus properties. *Nature, 338,* 334–337.
Gray, C. M., & Singer, W. (1989). Stimulus-specific neuronal oscillations in orientation columns of cat visual cortex. *Proceedings of the National Academy of Sciences, U.S.A., 86,* 1698–1702.
Greenamyre, J. T., Olson, J. M. M., Penney, J. B., & Young, A. B. (1985). Autoradiographic characterization of *N*-methyl-D-aspartate-quisqualate-sensitive and kainate-sensitive glutamate binding-sites. *Journal of Pharmacology and Experimental Therapeutics, 233,* 254–263.
Ho, N., & Destexhe, A. (2000). Synaptic background activity enhances the responsiveness of neocortical pyramidal neurons. *Journal of Neurophysiology, 84,* 1488–1496.
Hollmann, M., & Heinemann, S. (1994). Cloned glutamate receptors. *Annual Review of Neuroscience, 17,* 31–108.
Hopfinger, J. B., Buonocore, M. H., & Mangun, G. R. (2000). The neural mechanisms of top–down attentional control. *Nature Neuroscience, 3,* 284–291.
Jackson, M. E., & Cauller, L. J. (1998). Neural activity in SII modifies sensory evoked potentials in SI in awake rats. *NeuroReport, 9,* 3379–3382.
Jansen, B. H., & Brandt, M. E. (1991). The effect of the phase of prestimulus alpha-activity on the averaged visual evoked-response. *Electroencephalography and Clinical Neurophysiology, 80,* 241–250.
Jones, S. R., Pritchett, D. L., Stufflebeam, S. M., Hamalainen, M., & Moore, C. I. (2007). Neural correlates of tactile detection: A combined magnetoencephalography and biophysically based computational modeling study. *Journal of Neuroscience, 27,* 10751–10764.
Kaminski, M., Ding, M. Z., Truccolo, W. A., & Bressler, S. L. (2001). Evaluating causal relations in neural systems: Granger causality, directed transfer function and statistical assessment of significance. *Biological Cybernetics, 85,* 145–157.
Kastner, S., Pinsk, M. A., De Weerd, P., Desimone, R., & Ungerleider, L. G. (1999). Increased activity in human visual cortex during directed attention in the absence of visual stimulation. *Neuron, 22,* 751–761.
Klimesch, W., Sauseng, P., & Hanslmayr, S. (2007). EEG alpha oscillations: The inhibition-timing hypothesis. *Brain Research Reviews, 53,* 63–88.
Knight, R. T. (1997). Distributed cortical network for visual attention. *Journal of Cognitive Neuroscience, 9,* 75–91.
Knight, R. T., Staines, W. R., Swick, D., & Chao, L. L. (1999). Prefrontal cortex regulates inhibition and excitation in distributed neural networks. *Acta Psychologica, 101,* 159–178.
Kochan, L. D., Churn, S. B., Omojokun, O., Rice, A., & Delorenzo, R. J. (2000). Status epilepticus results in an *N*-methyl-D-aspartate receptor-dependent inhibition of Ca^{2+}/calmodulin-dependent kinase II activity in the rat. *Neuroscience, 95,* 735–743.
Kopell, N., Ermentrout, G. B., Whittington, M. A., & Traub, R. D. (2000). Gamma rhythms and beta rhythms have different synchronization properties. *Proceedings of the National Academy of Sciences, U.S.A., 97,* 1867–1872.
Kulics, A. T., & Cauller, L. J. (1986). Cerebral cortical somatosensory evoked-responses, multiple unit-activity and current source-densities—Their interrelationships and significance to somatic sensation as revealed by stimulation of the awake monkeys hand. *Experimental Brain Research, 62,* 46–60.
Lakatos, P., Chen, C. M., O'Connell, M. N., Mills, A., & Schroeder, C. E. (2007). Neuronal oscillations and multisensory interaction in primary auditory cortex. *Neuron, 53,* 279–292.
Lakatos, P., Karmos, G., Mehta, A. D., Ulbert, I., & Schroeder, C. E. (2008). Entrainment of neuronal oscillations as a mechanism of attentional selection. *Science, 320,* 110–113.
Lakatos, P., Shah, A. S., Knuth, K. H., Ulbert, I., Karmos, G., & Schroeder, C. E. (2005). An oscillatory hierarchy controlling neuronal excitability and stimulus processing in the auditory cortex. *Journal of Neurophysiology, 94,* 1904–1911.
Leek, M. R. (2001). Adaptive procedures in psychophysical research. *Perception & Psychophysics, 63,* 1279–1292.
Liang, H., Bressler, S. L., Ding, M., Truccolo, W. A., & Nakamura, R. (2002). Synchronized activity in prefrontal cortex during anticipation of visuomotor processing. *NeuroReport, 13,* 2011–2015.
Libet, B., Alberts, W. W., Wright, E. W., & Feinstei, B. (1967). Responses of human somatosensory cortex to stimuli below threshold for conscious sensation. *Science, 158,* 1597–1600.
Linkenkaer-Hansen, K., Nikulin, V. V., Palva, S., Ilmoniemi, R. J., & Palva, J. M. (2004). Prestimulus oscillations enhance psychophysical performance in humans. *Journal of Neuroscience, 24,* 10186–10190.
Luck, S. J. (2005). *An introduction to the event-related potential technique*. Cambridge, MA: MIT Press.

Makeig, S., Westerfield, M., Jung, T. P., Enghoff, S., Townsend, J., Courchesne, E., et al. (2002). Dynamic brain sources of visual evoked responses. *Science, 295,* 690–694.

Markram, H., Wang, Y., & Tsodyks, M. (1998). Differential signaling via the same axon of neocortical pyramidal neurons. *Proceedings of the National Academy of Sciences, U.S.A., 95,* 5323–5328.

McCarley, R. W., Faux, S. F., Shenton, M. E., Nestor, P. G., & Adams, J. (1991). Event-related potentials in schizophrenia—Their biological and clinical correlates and a new model of schizophrenic pathophysiology. *Schizophrenia Research, 4,* 209–231.

McCormick, D. A., Shu, Y. S., Hasenstaub, A., Sanchez-Vives, M., Badoual, M., & Bal, T. (2003). Persistent cortical activity: Mechanisms of generation and effects on neuronal excitability. *Cerebral Cortex, 13,* 1219–1231.

Meador, K. J., Ray, P. G., Echauz, J. R., Loring, D. W., & Vachtsevanos, G. J. (2002). Gamma coherence and conscious perception. *Neurology, 59,* 847–854.

Miller, E. K., & Cohen, J. D. (2001). An integrative theory of prefrontal cortex function. *Annual Review of Neuroscience, 24,* 167–202.

Mitra, P. P., & Pesaran, B. (1999). Analysis of dynamic brain imaging data. *Biophysical Journal, 76,* 691–708.

Nakajima, Y., & Imamura, N. (2000). Relationships between attention effects and intensity effects on the cognitive N140 and P300 components of somatosensory ERPs. *Clinical Neurophysiology, 111,* 1711–1718.

Newcomer, J. W., Farber, N. B., Jevtovic-Todorovic, V., Selke, G., Melson, A. K., Hershey, T., et al. (1999). Ketamine-induced NMDA receptor hypofunction as a model of memory impairment and psychosis. *Neuropsychopharmacology, 20,* 106–118.

Nikouline, V. V., Wikstrom, H., Linkenkaer-Hansen, K., Kesaniemi, M., Ilmoniemi, R. J., & Huttunen, J. (2000). Somatosensory evoked magnetic fields: Relation to pre-stimulus mu rhythm. *Clinical Neurophysiology, 111,* 1227–1233.

Nunez, P. L., Silberstein, R. B., Shi, Z. P., Carpenter, M. R., Srinivasan, R., Tucker, D. M., et al. (1999). EEC coherency: II. Experimental comparisons of multiple measures. *Electroencephalography and Clinical Neurophysiology, 110,* 469–486.

Nunez, P. L., Srinivasan, R., Westdorp, A. F., Wijesinghe, R. S., Tucker, D. M., Silberstein, R. B., et al. (1997). EEG coherency: I. Statistics, reference electrode, volume conduction, Laplacians, cortical imaging, and interpretation at multiple scales. *Electroencephalography and Clinical Neurophysiology, 103,* 499–515.

Okatan, M., Wilson, M. A., & Brown, E. N. (2005). Analyzing functional connectivity using a network likelihood model of ensemble neural spiking activity. *Neural Computation, 17,* 1927–1961.

Palva, S., Linkenkaer-Hansen, K., Näätänen, R., & Palva, J. M. (2005). Early neural correlates of conscious somatosensory perception. *Journal of Neuroscience, 25,* 5248–5258.

Palva, S., & Palva, J. M. (2007). New vistas for alpha-frequency band oscillations. *Trends in Neurosciences, 30,* 150–158.

Perrin, F., Pernier, J., Bertrand, O., & Echallier, J. F. (1989). Spherical splines for scalp potential and current-density mapping. *Electroencephalography and Clinical Neurophysiology, 72,* 184–187.

Petersen, C. C. H. (2002). Short-term dynamics of synaptic transmission within the excitatory neuronal network of rat layer 4 barrel cortex. *Journal of Neurophysiology, 87,* 2904–2914.

Petersen, C. C. H., Hahn, T. T. G., Mehta, M., Grinvald, A., & Sakmann, B. (2003). Interaction of sensory responses with spontaneous depolarization in layer 2/3 barrel cortex. *Proceedings of the National Academy of Sciences, U.S.A., 100,* 13638–13643.

Pfurtscheller, G., Neuper, C., Andrew, C., & Edlinger, G. (1997). Foot and hand area mu rhythms. *International Journal of Psychophysiology, 26,* 121–135.

Pineda, J. A. (2005). The functional significance of mu rhythms: Translating "seeing" and "hearing" into "doing". *Brain Research Reviews, 50,* 57–68.

Posner, M. I., & Petersen, S. E. (1990). The attention system of the human brain. *Annual Review of Neuroscience, 13,* 25–42.

Rajagovindan, R., & Ding, M. (2008). Decomposing neural synchrony: Toward an explanation for near-zero phase-lag in cortical oscillatory networks. *PLoS One, 3,* e3649.

Reyes, A., Lujan, R., Rozov, A., Burnashev, N., Somogyi, P., & Sakmann, B. (1998). Target-cell-specific facilitation and depression in neocortical circuits. *Nature Neuroscience, 1,* 279–285.

Rossi, A. F., Bichot, N. P., Desimone, R., & Ungerleider, L. G. (2007). Top–down attentional deficits in macaques with lesions of lateral prefrontal cortex. *Journal of Neuroscience, 27,* 11306–11314.

Salenius, S., Schnitzler, A., Salmelin, R., Jousmaki, V., & Hari, R. (1997). Modulation of human cortical Rolandic rhythms during natural sensorimotor tasks. *Neuroimage, 5,* 221–228.

Salin, P. A., & Bullier, J. (1995). Corticocortical connections in the visual-system—Structure and function. *Physiological Reviews, 75,* 107–154.

Salmelin, R., & Hari, R. (1994). Spatiotemporal characteristics of sensorimotor neuromagnetic rhythms related to thumb movement. *Neuroscience, 60,* 537–550.

Schaefer, A. T., Angelo, K., Spors, H., & Margrie, T. W. (2006). Neuronal oscillations enhance stimulus discrimination by ensuring action potential precision. *PLoS Biology, 4,* 1010–1024.

Scherg, M., Ille, N., Bornfleth, H., & Berg, P. (2002). Advanced tools for digital EEG review: Virtual source montages, whole-head mapping, correlation, and phase analysis. *Journal of Clinical Neurophysiology, 19,* 91–112.

Schubert, R., Blankenburg, F., Lemm, S., Villringer, A., & Curio, G. (2006). Now you feel it–Now you don't: ERP correlates of somatosensory awareness. *Psychophysiology, 43,* 31–40.

Shu, Y. S., Hasenstaub, A., Badoual, M., Bal, T., & McCormick, D. A. (2003). Barrages of synaptic activity control the gain and sensitivity of cortical neurons. *Journal of Neuroscience, 23,* 10388–10401.

Silva, L. R., Amitai, Y., & Connors, B. W. (1991). Intrinsic oscillations of neocortex generated by layer-5 pyramidal neurons. *Science, 251,* 432–435.

Staines, W. R., Graham, S. J., Black, S. E., & McIlroy, W. E. (2002). Task-relevant modulation of contralateral and ipsilateral primary somatosensory cortex and the role of a prefrontal–cortical sensory gating system. *Neuroimage, 15,* 190–199.

Taylor-Clarke, M., Kennett, S., & Haggard, P. (2002). Vision modulates somatosensory cortical processing. *Current Biology, 12,* 233–236.

Thomson, D. J. (1982). Spectrum estimation and harmonic-analysis. *Proceedings of the IEEE, 70,* 1055–1096.

Tomberg, C., & Desmedt, J. E. (1996). Non-averaged human brain potentials in somatic attention: The short-latency cognition-related P-40 component. *Journal of Physiology (London), 496,* 559–574.

Truccolo, W., Eden, U. T., Fellows, M. R., Donoghue, J. P., & Brown, E. N. (2005). A point process framework for relating neural spiking activity to spiking history, neural ensemble, and extrinsic covariate effects. *Journal of Neurophysiology, 93,* 1074–1089.

Vertes, R. P. (2005). Hippocampal theta rhythm: A tag for short-term memory. *Hippocampus, 15,* 923–935.

von Stein, A., Chiang, C., & Konig, P. (2000). Top–down processing mediated by interareal synchronization. *Proceedings of the National Academy of Sciences, U.S.A., 97,* 14748–14753.

Waberski, T. D., Gobbele, R., Darvas, F., Schmitz, S., & Buchner, H. (2002). Spatiotemporal imaging of electrical activity related to attention to somatosensory stimulation. *Neuroimage, 17,* 1347–1357.

Wiener, N. (1956). The theory of prediction. In *Modern mathematics for engineers*. New York: McGraw-Hill.

Wikstrom, H., Huttunen, J., Korvenoja, A., Virtanen, J., Salonen, O., Aronen, H., et al. (1996). Effects of interstimulus interval on somatosensory evoked magnetic fields (SEFs): A hypothesis concerning SEF generation at the primary sensorimotor cortex. *Evoked Potentials—Electroencephalography and Clinical Neurophysiology, 100,* 479–487.

Zhang, Y., Wang, X., Bressler, S. L., Chen, Y., & Ding, M. (2008). Prestimulus cortical activity is correlated with speed of visuomotor processing. *Journal of Cognitive Neuroscience, 20,* 1915–1925.

Zucker, R. S., & Regehr, W. G. (2002). Short-term synaptic plasticity. *Annual Review of Physiology, 64,* 355–405.